URTeC 2435418

Optimizing Unconventional Field Development through an Integrated Reservoir Characterization and Simulation Approach

Hasan Shojaei*, MicroSeismic, Inc.; Casey Lipp, Peregrine Petroleum

 DOI 10.15530-urtec-2016-2435418

This paper was prepared for presentation at the Unconventional Resources Technology Conference held in San Antonio, Texas, USA, 1-3 August 2016.

Abstract

In this paper we present the workflow, and a case study, for optimizing wellbore spacing and completion design in unconventional reservoirs by integrating reservoir characterization techniques with numerical reservoir simulation. The case study is from a pilot project for which extensive microseismic, core, PVT, and well-log data have been collected and analyzed. The pilot project includes two horizontal wells targeting the Cleveland formation in Oklahoma, with wellbore spacing that increases from 750 ft at the heel to 1,500 ft at the toe. Different completion designs (e.g. stage length, and number of perforation clusters per stage) have been used for the two wells.

A discrete fracture network (DFN) was constructed from the location, magnitude and focal mechanism of the captured microseismic events, which are assumed to represent rock failure caused by hydraulic stimulation. The proppant volume pumped at each stage was then distributed into the DFN to obtain a subset of the total DFN that is likely to be propped. This allows for the application of different compaction curves (i.e. conductivity reduction due to pressure drop from depletion) for propped and un-propped fractures in the model. The DFN model was then integrated with petro-physical well logs, core data, interpreted horizons, and PVT lab measurements to build a detailed reservoir model. Permeability enhancement in x-, y-, and z-direction was estimated based on the number of fractures, their orientation and geometry in each cell of the reservoir grid. History matching of production data was subsequently performed to calibrate the reservoir model. The reservoir drainage pattern obtained from the history-matched model was used to determine the optimum wellbore spacing, as well as the preferred completion design for different scenarios of oil price.

The reservoir model obtained in this work captures the variations in fracture geometry and intensity along the wellbore, which is fundamentally different from traditional models that assume bi-wing fractures with uniform fracture spacing, half-length and conductivity along the wellbore. The quantified permeability enhancement for each cell, and the subsequent reservoir drainage pattern obtained from reservoir simulation, provide a success measure for treatment design of each stage, as well as the spacing among the wells.

Introduction

Microseismic monitoring of hydraulic fracturing treatment has found growing number of applications in recent years. What started as a technique to merely map the locations of induced fractures has grown into a technology that provides invaluable information about the mechanisms of the fracturing process, as well as the underlying geologic formation. For example, several investigators have used moment tensor inversion and source mechanism analysis to extract information about the orientation and slip direction of failed fracture planes (e.g. Vavryčuk, 2007; Williams-Stroud et al., 2010; Warpinski and Du, 2010; Williams-Stroud and Eisner, 2014). Microseismic source mechanisms have also been used to determine the orientation and magnitude of horizontal field stresses (e.g. Stanek et al., 2015; Agharazi, 2016).

Transient development of the microseismic cloud has been used to estimate a system or bulk permeability for the stimulated reservoir (e.g. Shapiro et al., 2002; Shapiro and Dinske, 2009). Others have used microseismic data to assess geohazards (e.g. Snelling et al., 2013; Jabbari et al., 2015), evaluate diverters (Waters et al., 2009; Diakhate et al., 2015), and link the effectiveness of hydraulic fracture treatment to structural features of the reservoir (e.g. Rich and Ammerman, 2010; Meek et al., 2013).

Microseismic data have been widely used to evaluate wellbore and stage spacing during unconventional field development. However, this has been mainly done in a purely geometrical sense, i.e. by measuring the degree of overlap between microseismic clouds of two neighboring wells or stages. Even though this approach provides valuable information about the stimulated rock volume (SRV) for each well or stage, it does not take into account flow properties of the reservoir rock and fluid, nor pressure management of individual wells, which together dominate fluid flow in the reservoir and the resulting reservoir depletion.

In this paper we propose a workflow, and a case study, in which microseismic data are integrated with treatment, core, well-log, PVT, and relative permeability data, as well as the interpreted horizons from 3D seismic to build a detailed reservoir simulation model. The constructed reservoir model is calibrated by performing history matching of production data. The reservoir drainage pattern obtained from the history-matched model is used to determine the optimum wellbore spacing, and the preferred completion design based on different scenarios of oil price.

The reservoir simulation model obtained in this work captures the variations in fracture geometry (i.e. azimuth, dip angle, dimensions) and intensity (i.e. number of fractures per unit length) along and away from the wellbore. This is fundamentally different from traditional reservoir models that assume simple fractures with uniform fracture spacing, half-length and conductivity along the wellbore. Rate-transient analysis (RTA), which is frequently used to evaluate wellbore spacing by estimating the effective fracture half-length and conductivity, is limited by the same simplifying assumptions about fracture geometry as the traditional reservoir simulation models. Such simple fracture models do not represent the complex network of fractures that are created in the reservoir due to interactions between hydraulic fractures and pre-existing natural fractures and faults.

Optimizing wellbore spacing and completion design is a key step towards successful development of unconventional resource plays. Understanding the reservoir drainage pattern of each well can prevent incorrect spacing of wells, which may result in wells competing for the same drainage volume, or significant volumes of rock being left undrained. Predicting accurate reservoir drainage patterns also enables the optimization of other field development variables such as stage lengths and spacing, clustering, or re-fracturing.

Methodology

Microseismic data are combined with treatment information to construct a deterministic DFN that represents the fracture network that is created in the reservoir during hydraulic fracturing treatment. Each microseismic event is assumed to originate from slippage along an individual fracture. The orientation (i.e. azimuth and dip angle) of each fracture in the DFN is determined by the event's focal mechanism; and its size is obtained from the magnitude of the event, rock rigidity, injected fluid volumes and fluid efficiency. The injected proppant volume is then distributed into the DFN using a mass balance approach to obtain a subset of the total DFN that is likely to be propped. Figure 1 depicts the microseismic events captured during hydraulic stimulation of the two wells from the case study that will be presented in this paper. The events are color-coded by stage number, and sized by the event magnitude. The corresponding total DFN and propped-DFN are shown in Figure 2.

As mentioned earlier, this approach differentiates between proppant-filled and un-propped fractures. The reservoir volume affected by the total DFN is called the Stimulated Rock Volume (SRV), while the reservoir volume affected by the proppant-filled fractures is referred to as the Productive Stimulated Rock Volume (P-SRV), as the proppant-filled fractures are expected to remain open and contribute to production more effectively. A detailed explanation of this deterministic DFN process can be found in McKenna et al. (2015).

One key advantage of this approach is the ability to capture the fracture intensity (number of fractures, their orientation and aperture) achieved in each cell of the reservoir grid. This fracture intensity can be translated into a permeability tensor using the approach of Oda, (1985), providing quantification of the unscaled permeability enhancement in x-, y-, and z-direction in each cell.

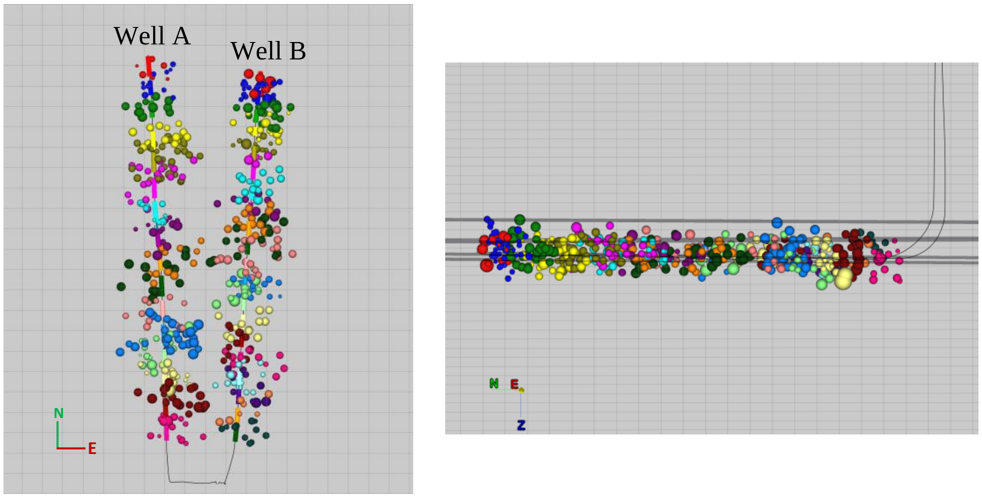

Figure 1: Microseismic events in map view (left) and depth view (right). Events are color-coded by stage number and sized by event magnitude. The background grid is 250 ft × 250 ft in the map view, while it is 250 ft × 100 ft in the depth view.

We use the permeability enhancement results as each cell's comparative magnitude of permeability. In other words, the permeability enhancement results demonstrate the amount of permeability enhancement in each cell compared to its neighboring cell. Figure 3 depicts the distribution of permeability enhancement in x-direction (perpendicular to the wells) within SRV and P-SRV of the case study that will be discussed in the next section. In this figure warm colors represent large permeability enhancement, while cool colors indicate small permeability enhancement.

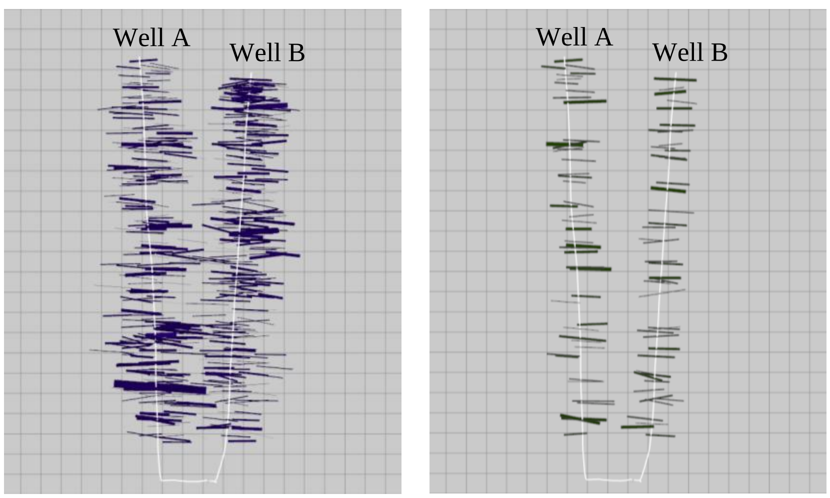

Figure 2: Total DFN (left) and propped-DFN (right). The background grid is 250 ft × 250 ft.

The permeability enhancement results, obtained from the microseismic-derived DFN, are combined with other available data to construct a detailed reservoir simulation model. The reservoir rock properties in each layer of the reservoir model (i.e. porosity, initial water saturation, net pay, matrix permeability) are specified based on core data, petro-physical well logs, and interpreted horizons. Fluid properties and rock-fluid interactions are defined based on PVT and relative permeability measurements respectively.

The model is then calibrated by performing history-matching of production data. An identical permeability multiplier is applied to all the P-SRV cells, while a separate permeability multiplier is applied to the cells located in the un-propped portion of the SRV. Differentiating between propped and un-propped fractures also allows for the application of different compaction curves for propped and un-propped fractures in the model. The history matching process is continued until a reasonable agreement between simulation results and field data is achieved. The resulting reservoir drainage pattern is used to determine the optimum wellbore spacing, as well as the preferred completion design.

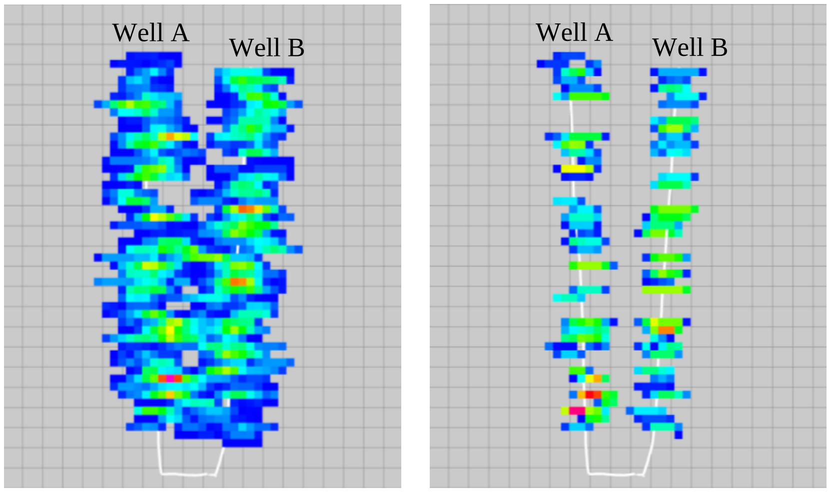

Figure 3: Distribution of permeability enhancement within SRV (left) and P-SRV (right). Warm (cool) colors represent large (small) permeability enhancement. The background grid is 250 ft × 250 ft, while the SRV and P-SRV cells are 100 ft × 100 ft.

Cleveland Formation Case Study

The case study is from a pilot project in Ellis County, Oklahoma, in which two horizontal wells are drilled and completed in the early Missourian Cleveland formation. The reservoir is interpreted as being dominated by low-permeability tidal-shelf and distal delta-front deposits. These lenticular sand bodies make it difficult to predict the size and distribution of the reservoir and, therefore, the potential per-well reserves.

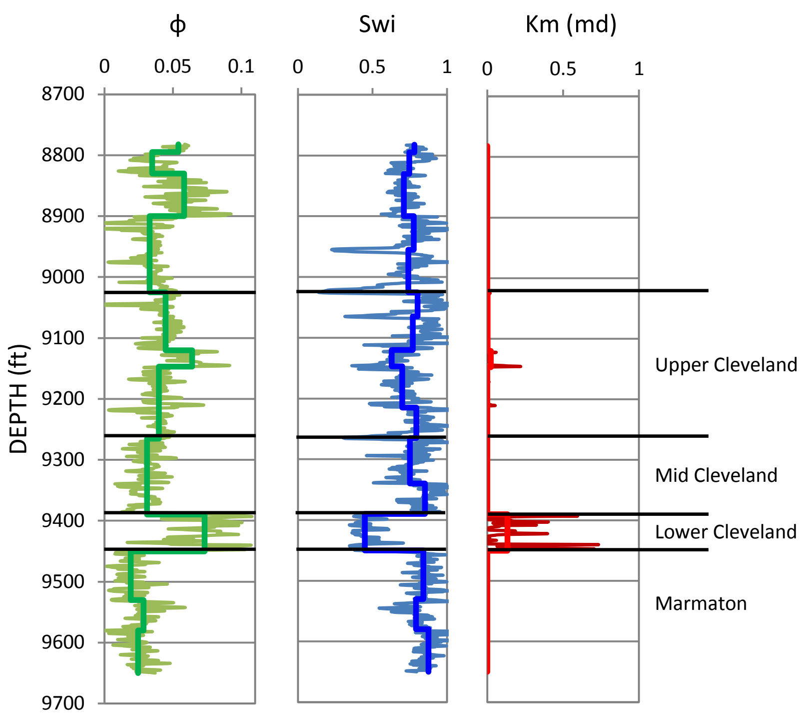

Figure 4: Variations in porosity, initial water saturation and matrix permeability with depth.

The incised, valley-filled depositional environment makes for highly variable geology, and poses challenges in determining the optimum wellbore spacing and completion design. To address these challenges, a pilot project with two horizontal wells was carried out in which the wellbore spacing increased from 750 ft at the heel to 1,500 ft at the toe; and different completion designs (i.e. stage length, and number of perforation clusters per stage) were used for each well.

Extensive 3D seismic, well-log and core data had been collected and analyzed for the area in which the pilot project was carried out. Figure 4 shows the variations in effective porosity, initial water saturation and matrix permeability with depth for the two wells in consideration. The reservoir rock properties in each layer of the reservoir model were specified based on the data shown in Figure 4. The average effective porosity in the pay zone (i.e. Lower Cleveland) is 7.3%, while the average initial water saturation and matrix permeability in the pay zone are 45% and 0.09 md respectively.

A black-oil reservoir model (e.g. Trangenstein and Bell, 1989; Coats et al., 1998; Elahi and Jafarpour, 2015) was used throughout this study. The PVT lab measurements (Figure 5) were used to specify reservoir fluid properties in the model. The bubble point pressure of the reservoir oil is approximately 2,000 psi at reservoir temperature of 185 ˚F. The initial pore pressure in the pay zone was measured to be nearly 4,100 psi. The Stone II model (Stone, 1973; Nomeli and Riaz, 2015) was used to represent three-phase flow conditions in the reservoir. The water-oil and gas-oil relative permeability functions were specified based on our knowledge of the Cleveland formation.

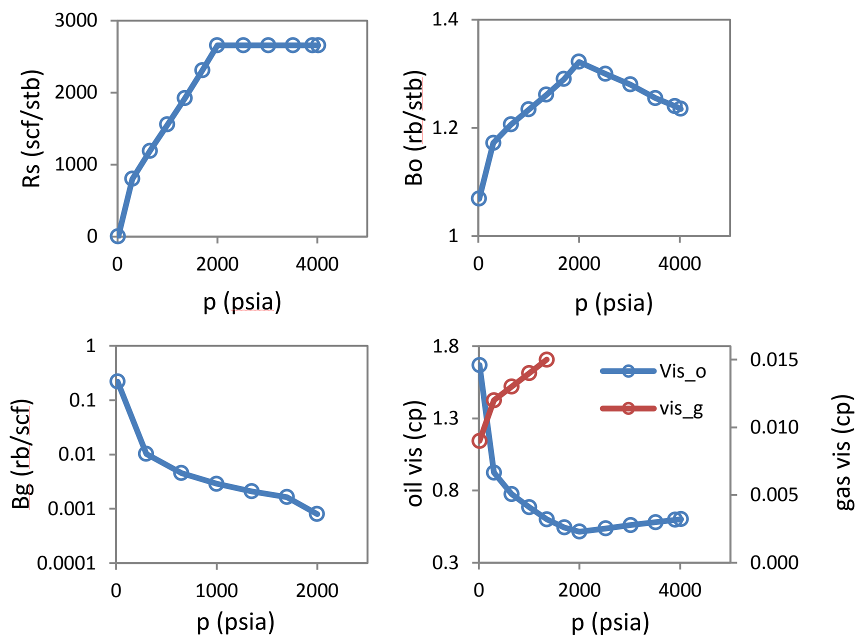

Figure 5: Solution gas-oil ratio (top left); Oil formation volume factor (top right); Gas formation volume factor (bottom left); and oil and gas viscosities (bottom right).

Microseismic data had been collected during hydraulic fracturing treatment using a temporary surface array (Figure 1). A DFN representing the induced hydraulic fractures, and possibly re-activated natural fractures, was constructed and populated with proppant using the methodology described in earlier sections (Figure 2). Permeability enhancement in x-, y-, and z-direction due to hydraulic fracturing was then estimated in each grid cell of the reservoir model using the Oda approach (Figure 3). For this case study, it was assumed that un-propped fractures are closed immediately after flowback. Therefore the permeability enhancement in the un-propped portion of SRV was neglected during reservoir simulation.

The measured wellhead pressure (WHP) profile was used as input to the reservoir simulator to calculate oil, gas and water production rates. The bottomhole pressure (BHP) values were calculated from WHP using the Drift-Flux model (Shi et al., 2005; Frooqnia, 2014) inside the simulator (CMG IMEX, 2015). The reservoir simulation model was calibrated by matching the calculated oil rates to the actual measurements. During the history matching process, an identical permeability multiplier was applied to all the cells within the P-SRV until a reasonable agreement between simulation results and field data was obtained. The reduction in fracture conductivity due to pressure depletion was accounted for by applying a compaction table to the cells within P-SRV.

A very good agreement between simulation results and actual oil rates was obtained for both wells A and B (Figure 6). It should be noted that different completion designs have been used for these two wells. Well A was fractured in 16 stages while well B was fractured in 20 stages. In other words smaller stage length and spacing were used for well B, while similar amounts of water and proppant were pumped into these two wells. That is, smaller amounts of water and proppant per stage were pumped for well B.

The aforementioned differences in completion design have led to different production profiles for these two wells. Well B exhibits a higher initial production (IP) followed by a faster decline compared to well A. These differences in IP and decline behavior of the two wells, which is accurately captured by the model, can have significant implications for unconventional field development depending on the prevailing economic conditions. For example in a high oil price environment the operator may want to accelerate oil production, and therefore prefer the completion design of well B. On the other hand, the completion design of well A may be preferred at low oil prices, as the operator may want to wait longer until oil prices recover.

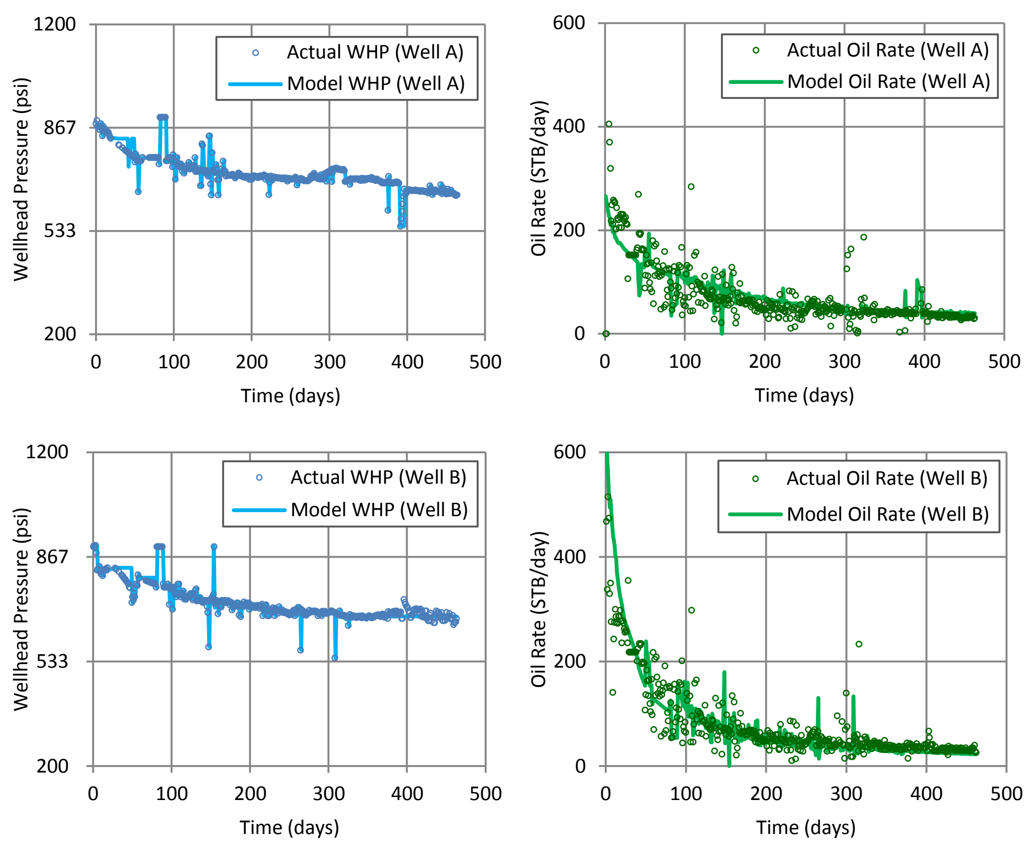

Figure 6: WHP profile for well A (top left); Oil rates for Well A (top right); WHP profile for well B (bottom left); Oil rates for Well B (bottom right).

The analysis of pressure depletion in the reservoir provides a unique tool for evaluating and optimizing wellbore spacing in unconventional reservoirs. Figure 7 shows how pressure distribution in the pay zone evolves with time based on the history-matched reservoir model. If we base our calculation of optimum wellbore spacing on the pressure depletion map at 12 months into production, the optimum wellbore spacing will be approximately 1,100 ft, where the two wells interfere with a pressure drop of nearly 650 psi in the reservoir.

The 12-month pressure depletion map was chosen as the reference because the first year is the most important period during the lifetime of an unconventional well. Most unconventional wells produce a large portion of their expected EUR during the initial 12 months. The two wells in this case study have produced nearly 40% of their expected combined EUR during the initial 12 months. The EUR values for these two wells were calculated by assuming a WHP profile and performing reservoir simulation for the next 30 years. Similar EUR values were obtained when we performed decline curve analysis (DCA) based on the approach of Duong, (2011).

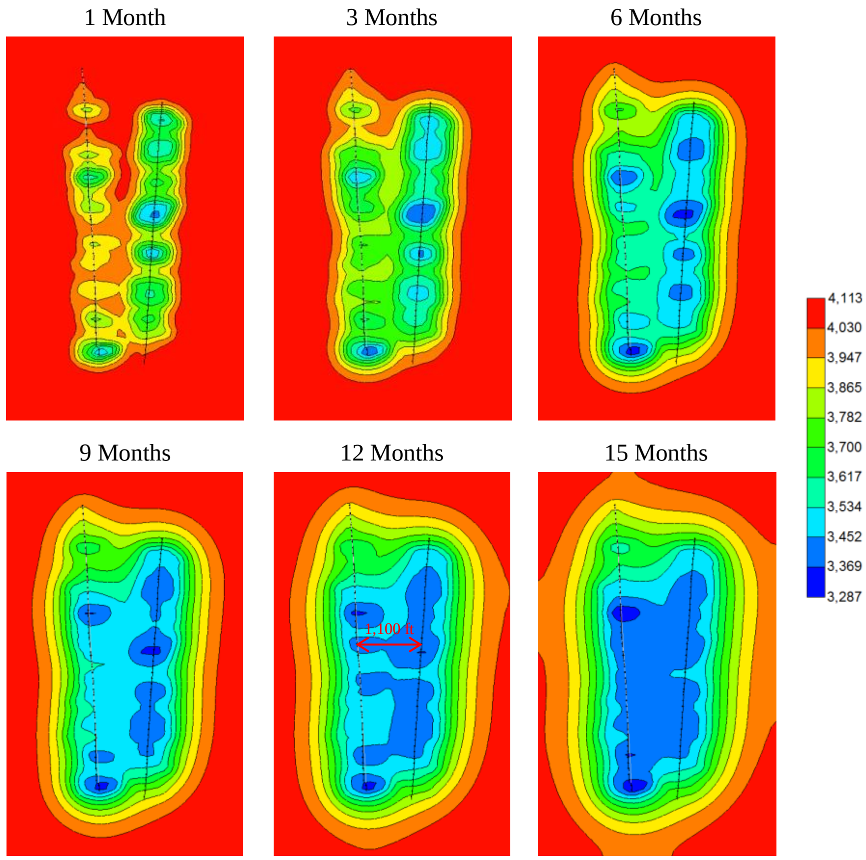

Figure 7: Pressure distribution (psi) in the pay zone at 1 month, 3 months, 6 months, 9 months, 12 months and 15 months into production.

Conclusions

There is a significant gap in the industry's ability to measure the reservoir's reaction to hydraulic fracturing and, therefore, it is difficult to predict future production and the resulting drainage patterns in the reservoir. This has made the optimization of unconventional field development very challenging.

In this paper we presented a workflow that integrates microseismic data with treatment, core, well-log, PVT, and relative permeability data to arrive at a detailed reservoir simulation model that captures the variations in fracture geometry and intensity along and away from the wellbore, as well as the flow properties of reservoir rock and fluid. This is fundamentally different from traditional models that assume unrealistic fracture geometries leading to inaccurate predictions of unconventional wells' production and drainage patterns.

The proposed methodology was applied to two horizontal wells with wellbore spacing that increased from 750 ft at the heel to 1,500 ft at the toe. The reservoir model was able to accurately capture the differences between initial production and decline behavior of the two wells, which had been completed differently. The reservoir simulation results were used to determine the optimum wellbore spacing, as well as the preferred completion design for different scenarios of oil price.

The approach presented in this work provides a unique solution for understanding the reservoir after hydraulic fracturing treatment. The quantified permeability enhancement enables completion and reservoir engineers to assess the success of a hydraulic fracture job and reliably estimate the productivity of a well shortly after the treatment.

Acknowledgement

The authors would like to thank Peregrine Petroleum for permission to publish the results presented in this paper.

References

Agharazi, A. 2016. Determination of Maximum Horizontal Field Stress from Microseismic Focal Mechanisms – A Deterministic Approach. Paper ARMA 15-514 presented at the 50th US Rock Mechanics / Geomechanics Symposium, Houston, TX, USA, June 26-29.

CMG-IMEX. Three-Phase, Black-Oil Reservoir Simulator. Version 2015 User's Guide. Computer Modeling Group Ltd., Calgary, Alberta, Canada.

Coats, K.H., Thomas, L.K., Pierson, R.G. 1998. Compositional and Black Oil Reservoir Simulation. SPE Reservoir Evaluation & Engineering **1**(04): 372-379.

Diakhate, M., Gazawi, A., Barree, R.D., Cossio, M., Tinnin, B., McDonald, B., Barzola, G. 2015. Refracturing on Horizontal Wells in the Eagle Ford Shale in South Texas-One Operator's Perspective. Paper SPE 173333 presented at the SPE Hydraulic Fracturing Technology Conference, The Woodlands, Texas, USA, 3-5 February.

Duong, A.N. 2011. Rate-Decline Analysis for Fracture-Dominated Shale Reservoirs. SPE Reservoir Evaluation & Engineering **14**(03): 377-387.

Elahi, S.H., Jafarpour, B. 2015. Characterization of Fracture Length and Conductivity from Tracer Test and Production Data with Ensemble Kalman Filter. Unconventional Resources Technology Conference (URTeC), San Antonio, Texas, USA, 20-22 July. doi:10.2118/178707-MS

Frooqnia, A. 2014. Numerical Simulation and Interpretation of Borehole Fluid-Production Measurements. Ph.D. Dissertation, University of Texas at Austin, Austin, Texas, USA.

Jabbari, N., Ashayeri, C., Meshkati, N. 2015. Leading Safety, Health, and Environmental Indicators in Hydraulic Fracturing. Paper SPE 174059 presented at the SPE Western Regional Meeting, Garden Grove, California, USA, 27-30 April.

McKenna, J.P., Quezada, O., Toohey, N.M., Grealy, M.H. 2015. A Data-Driven Proppant-Filled Fracture Model: Comparing Sliding Sleeve and Plug and Perf Completion Styles. SEG Annual Meeting, New Orleans, Louisiana, USA, 18-23 October.

Meek, R., Suliman, B., Hull, R., Bello, H., Portis, D. 2013. What Broke? Microseismic Analysis using Seismic Derived Rock Properties and Structural Attributes in the Eagle Ford Play. Unconventional Resources Technology Conference (URTeC), Denver, Colorado, USA, 12-14 August.

Nomeli, M.A., Riaz, A. 2015. The Potential for Carbon Dioxide Sequestration in Subsurface Geological Formations. Handbook of Clean Energy Systems. 1–10.

Oda, M. 1985. Permeability Tensor for Discontinuous Rock Masses. Geotechnique **35**(4): 483-495.

Rich, J.P., Ammerman, M. 2010. Unconventional Geophysics for Unconventional Plays. Paper SPE 131779 presented at the SPE Unconventional Gas Conference, Pittsburgh, Pennsylvania, USA, 23-25 February.

Shapiro, S.A., Dinske, C. 2009. Fluid-Induced Seismicity: Pressure Diffusion and Hydraulic Fracturing. Geophysical Prospecting **57**(2): 301-310.

Shapiro, S.A., Rothert, E., Rath, V., Rindschwentner, J. 2002. Characterization of Fluid Transport Properties of Reservoirs using Induced Microseismicity. Geophysics **67**(1): 212-220.

Shi, H., Holmes, J.A., Durlofsky, L.J., Aziz, K., Diaz, L., Alkaya, B., Oddie, G. 2005. Drift-Flux Modeling of Two-Phase Flow in Wellbores. SPE Journal **10**: 24-33. doi:10.2118/84228-PA

Snelling, P., de Groot, M., Craig, C., Hwang, K. 2013. Structural Controls on Stress and Microseismic Response - A Horn River Basin Case Study. Paper SPE 167132 presented at the SPE Unconventional Resources Conference Canada, Calgary, Alberta, Canada, 5-7 November. doi:10.2118/167132-MS

Staněk, F., Jechumtálová, Z., Eisner, L., 2015. Reservoir Stress from Microseismic Source Mechanisms. The Leading Edge **34**(8): 890-895.

Stone, H.L. 1973. Estimation of Three-Phase Relative Permeability and Residual Oil Data. J. Pet. Technol. **12**(4).

Trangenstein, J.A., Bell, J.B. 1989. Mathematical Structure of the Black-Oil Model for Petroleum Reservoir Simulation. SIAM Journal on Applied Mathematics **49**(3): 749-783.

Vavryčuk, V. 2007. On the Retrieval of Moment Tensors from Borehole Data. Geophysical Prospecting **55**: 381–391. doi: 10.1111/j.1365-2478.2007.00624.x

Warpinski, N.R., Du, J. 2010. Source-Mechanism Studies on Microseismicity Induced by Hydraulic Fracturing. Presented at the SPE Annual Technical Conference and Exhibition, Florence, Italy, 19-22 September.

Waters, G., Ramakrishnan, H., Daniels, J., Bentley, D., Belhadi, J., Ammerman, M. 2009. Utilization of Real Time Microseismic Monitoring and Hydraulic Fracture Diversion Technology in the Completion of Barnett Shale Horizontal Wells. Presented at the Offshore Technology Conference, Houston, Texas, USA, 4-7 May.

Williams-Stroud, S.C., Eisner, L., Microseismic, Inc. 2014. Method for Determining Discrete Fracture Networks from Passive Seismic Signals and Its Application to Subsurface Reservoir Simulation. U.S. Patent 8,902,710.

Williams-Stroud, S.C., Kilpatrick, J.E., Cornette, B., Eisner, L., Hall, M. 2010. Moving Outside of the Borehole: Characterizing Natural Fractures through Microseismic Monitoring. First Break **28**(7).